

Design of Slotted Permanent Magnet Linear Synchronous Motor for Improved Thrust Density

Nariman Roshandel Tavana, *Student Member, IEEE*, and Venkata Dinavahi, *Senior Member, IEEE*

Abstract— Since a linear motor with high thrust density and low thrust ripple is desired for many industrial applications, in this paper, a design methodology is proposed to achieve these objectives. A slotted permanent magnet linear synchronous motor (SPMLSM) which inherently offers the highest force density among various types of linear motors is selected for analysis and optimization procedure. An analytical model is derived for the SPMLSM by solving Maxwell's equations for calculating the magnetic field and force. Motor dimensions are then optimized using the analytical model and genetic algorithm, where the increase of force density and the reduction of thrust ripple are considered as the optimization target. In this study, to reach a higher optimal point in the multidimensional search space of the machine design, cogging force caused by slot effect is initially neglected in the model. Subsequently, pole-shifting is applied to the optimal model to eliminate cogging force and satisfy design objectives. Finally, the effectiveness of the proposed technique to enhance motor performance is investigated by a time-stepping transient finite-element method. The results show an improvement in the performance of optimized motor.

Index Terms— Design optimization, finite-element method, genetic algorithm, permanent magnet linear synchronous motor.

NOMENCLATURE

J_M	Equivalent magnetization current vector
\mathbf{a}_y	Unit vector in y direction
H	Magnetic field intensity
B	Magnetic field density
L	Motor width
g	Mechanical air-gap length
k_{wn}	Winding factor of n th harmonic
p_f	Coil packing factor
P	Number of pole pairs
l_m	Magnet height
w_m	Magnet width
τ	Pole pitch
τ_{wp}	Winding pitch
J	Current density
B_r	Remanence
χ_0	Load angle

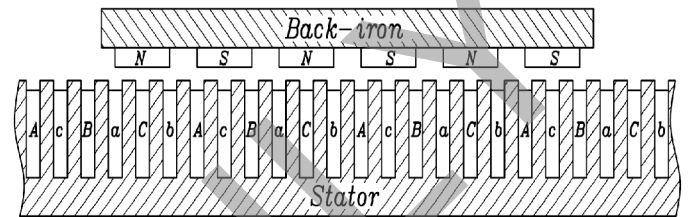


Fig.1. Topology of a single-sided SPMLSM.

I. INTRODUCTION

Linear motors are commonly used in industrial automation in all kinds of drive systems. In comparison with their rotary-to-linear counterparts, they offer higher dynamic performance, higher efficiency, and improved reliability due to the absence of gears and transmission systems [1-2]. Many researches have been done about the design of the linear motor with different objectives and targets. However, the design of a SPMLSM with high thrust density and low thrust ripple which is suitable for industrial automation gained less attention [3-6].

Among different types of linear motors, the SPMLSM benefits from the highest force density and efficiency as well as easy maintenance and simplicity of control. Nevertheless, it suffers from thrust fluctuation due mainly to the cogging force by slot effect and non-sinusoidal flux density distribution produced by the permanent magnet (PM) poles.

In this paper, an analytical model based on Maxwell's equations is presented for the modeling of SPMLSM. Then, a design optimization is carried out based on the analytical model and genetic algorithm to find the best set of motor dimensions to maximize thrust density and minimize thrust ripple regardless of cogging force (for the reduction of one constrain from optimization procedure) to achieve a higher optimal point from objective function point of view. Pole-shifting is then applied to the optimal configuration to reduce the cogging force considerably, while force density remained approximately the same. Finally, FEM is employed to confirm the effectiveness of design method.

II. ANALYTICAL MODELING OF SPMLSM

A. Machine Topology

This paper focuses on modeling and design optimization of a single-sided SPMLSM topology which is shown in Fig. 1 and whose parameters and specifications are listed in Table. I.

The authors are with the Department of Electrical and Computer Engineering, University of Alberta, Edmonton, AB T6G 2V4, Canada (e-mail: roshande@ualberta.ca; dinavahi@ualberta.ca).

Table I. Geometric parameters of the original SPMLSM.

Parameter	Value	Parameter	Value
Motor width (L)	83 (mm)	Magnet width (W_m)	14.7 (mm)
Pole pitch (τ)	24 (mm)	Tooth depth (T_h)	12 (mm)
Magnet height (l_m)	2.5 (mm)	Air-gap length (g)	1 (mm)
Armature current density (J)	$5 \left(\frac{A}{mm^2}\right)$	Tooth width (T_w)	4.5 (mm)

B. Field Distribution due to PM Source

In order to establish the analytical solution for the magnetic field distribution in the foregoing machine topology, the following assumptions are made [7]:

- 1) The length of the motor is extended to infinity,
- 2) The permeability of the iron core is infinite,
- 3) The PMs have a linear demagnetization characteristic, and their permeability is equal to the permeability of free space.

Consequently, the magnetic field analysis due to magnetic poles is confined to two layers: the air space/winding and the PM layer. The governing field equations in terms of the magnetic vector potential lead to Laplace and Poisson equations as follows [8]:

$$\begin{cases} \nabla^2 A_I = 0 & \text{in air gap layer,} \\ \nabla^2 A_{II} = -\mu_0 J_M & \text{in PM layer.} \end{cases} \quad (1)$$

where $J_M = \nabla \times \mathbf{M}$ and \mathbf{M} is the magnetization vector of the i th magnetic segment given by

$$\mathbf{M} = M_y \mathbf{a}_y \quad (2)$$

where M_{y_i} denotes the component of \mathbf{M}_i in y direction. The distribution of M_{y_i} can be expressed as the Fourier series

$$M_y = \sum_{n=1,3,\dots}^{\infty} P_n \sin\left(\frac{m_n W_m}{2}\right) \cos(m_n x) \quad (3)$$

where $P_n = \frac{4B_r}{n\pi\mu_0}$ and $m_n = \frac{n\pi}{\tau}$. The boundary conditions to be satisfied by the solution to (1) are

$$\begin{cases} H_{Ix}|_{y=g_c} = 0; & H_{IIx}|_{y=-l_m} = 0 \\ H_{Ix}|_{y=0} = H_{IIx}|_{y=0}; & B_{Iy}|_{y=0} = B_{IIy}|_{y=0} \end{cases} \quad (4)$$

where g_c is the modified air-gap length with Carter coefficient (K_c) for slotted stator structure.

$$g_c = K_c g \quad (5)$$

By solving (1), the tangential and normal components (B_x and B_y) of the flux density produced by PM in the air gap are provided from the curl of \mathbf{A}_I as follows:

$$B_{Ix}(x, y) = - \sum_{n=1,3,\dots}^{\infty} m_n [a_{In} \sinh(m_n y) + b_{In} \cosh(m_n y)] \sin(m_n x), \quad (6)$$

$$B_{Iy}(x, y) = \sum_{n=1,3,\dots}^{\infty} m_n [a_{In} \cosh(m_n y) + b_{In} \sinh(m_n y)] \cos(m_n x). \quad (7)$$

where a_{In} and b_{In} are determined as

$$a_{In_i} = \frac{(e^{m_n l_m} - e^{-m_n l_m})(e^{m_n l_g} - e^{-m_n l_g})}{(e^{m_n(l_g+l_m)} - e^{-m_n(l_g+l_m)})} \left(\frac{P_n \mu_0}{2m_n} \sin\left(\frac{m_n W_m}{2}\right) \right) \quad (8)$$

$$b_{In} = \frac{(e^{-m_n l_g} - e^{m_n l_g})}{(e^{m_n l_g} + e^{-m_n l_g})} a_{In} \quad (9)$$

C. Thrust Prediction

The thrust force exerted on the armature, resulting from the interaction between the current carried by conductors and the normal component of PM magnetic field, is the so-called Lorentz force \mathbf{F} which is given by

$$\mathbf{F} = \int_V \mathbf{J} \times \mathbf{B} dV \quad (10)$$

For a three-phase machine carrying balanced sinusoidal time-varying currents, the thrust force can be calculated from

$$F_{3ph}(x) = F_A(x) + F_B(x) + F_C(x), \quad (11)$$

$$F_{3ph}(x) = \frac{3}{2} T_1 \sin\left(\frac{\pi}{\tau} x_0\right) + \sum_{n=5,11,\dots}^{\infty} \frac{3}{2} T_n \cos\left(m_{n+1} x - m_n \frac{\tau_{wp}}{2} + m_n x_0\right) + \sum_{n=7,13,\dots}^{\infty} \frac{3}{2} T_n \cos\left(m_{n-1} x - m_n \frac{\tau_{wp}}{2} + m_n x_0\right). \quad (12)$$

Therefore, the average thrust force due to the magnetic poles is given by

$$F_{3ph_{avg}} = \frac{3}{2} T_1 \sin\left(\frac{\pi}{\tau} x_0\right) \quad (13)$$

D. Comparison with FEM

The validity of the analytical results for the calculation of magnetic field and thrust force in the SPMLSM depends on the accuracy of the model. However, the model is obtained by some simplification. Thus, it is necessary to evaluate the extent of model accuracy. In this section, a 2-D nonlinear time stepping transient finite-element method is employed to validate the model. The relative movement is taken into account in the FEM by using time stepping transient analysis and the Lagrange multiplier method [9].

Fig. 2 shows the comparisons between the normal component of open-circuit flux density distributions computed by the analytical method and FEM as functions of x position at the center of the mechanical air-gap. It can be seen that the analytical method can properly predict the magnetic field; however, the only difference is close to the slot openings not taken into account in the model.

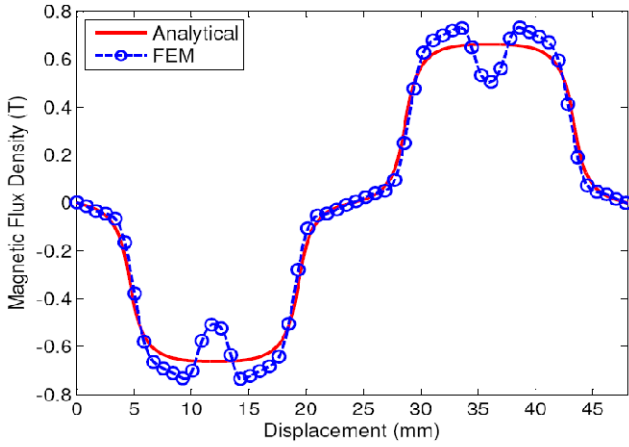


Fig. 2. Normal component of flux density distribution by PM.

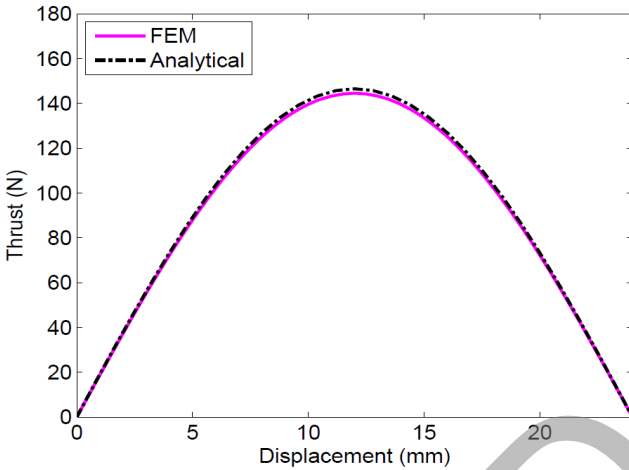


Fig. 3. Thrust characteristic of SPMLSM.

Fig. 3 compares the analytically predicted and FEM-calculated thrust force distribution with respect to the mover position. It is seen that the analytical prediction agrees well with the finite-element solution, the slight discrepancy is due mainly to the effect of core saturation, which is neglected in the analytical model.

III. OPTIMAL DESIGN OF SPMLSM

In this paper, genetic algorithm is applied to the design of SPMLSM to fulfill the objectives of design optimization. To maximize force density and minimize thrust ripple in SPMLSM, a widely used technique is to reduce the multiobjective optimization to a single objective one [10]. Thus, an augmented objective function is defined by combining the objectives as follows

$$OF(X) = \left(\frac{F_{3ph_{ave}}(X)}{V_{motor}(X)} \right) \cdot F_{3ph_{ripple}}^{-1}(X) \quad (14)$$

A genetic algorithm with parameters listed in Table. II is employed to maximize the objective function. Motor dimensions are chosen as the optimization variables. To have a more realistic design, some limitations are applied to the optimization procedure as shown in Table. III. Finally, in the optimal models, the SPMLSM dimensions using genetic algorithm are calculated and listed in Table. IV.

Table. II. Genetic algorithm parameters.

Parameter	Value
Initial population	50
Probability of mutation	0.07
Probability of crossover	0.07
Number of generations	1000

Table. III. Design variables and constraints.

Parameter (unit)	Min. Value	Max. Value
g (mm)	1	1.7
l_m (mm)	2	4
W_m (mm)	10	24
T_w (mm)	2.5	5.5
T_h (mm)	8	16
L (mm)	75	85
F_{avg} (N)	145	155

Table. IV. Optimal motor parameters.

Parameter (unit)	Value
g (mm)	1.5
l_m (mm)	2.3
W_m (mm)	19.5
T_w (mm)	4.7
T_h (mm)	12.8
L (mm)	75.1

It is worth mentioning that the thrust ripple due to harmonics of flux density distribution of permanent magnets is taken into account for modeling and design optimization; however, the cogging force caused by slot effects is neglected. Pole-shifting as an extra degree of freedom in the design procedure is applied to the optimized model to eliminate cogging force substantially and enhance its performance while the force density is reduced slightly.

It should also be noted that the technique of pole-shifting consists of shifting each PM by a quantity of Δx [11], so that the cogging force of various poles are not in phase and its total value is strongly reduced.

IV. DESIGN EVALUATION

The performance of the optimized SPMLSM is investigated and compared with the performance of the initial SPMLSM. Since an optimization procedure based on the analytical method has been employed to determine the optimal design specifications, another more accurate method, for example FEM, should be used to assess the performance of the optimized motor.

FEM results for the investigation of analyzed motors are shown in Table. V. It can be seen that the force density increases by 11.6% in the optimized model with respect to initial one and after pole-shifting, it increases by 8.61%.

A comparison of FEM-calculated thrust force which results from the rated three-phase sinusoidal current excitation is given in Fig. 4. It can be observed that thrust ripple is reduced by 39.72% in the optimal configuration and 95.11% in the optimized model with pole-shifting compared with original one.

The FEM-calculated thrust force distribution with respect to the mover position is depicted in Fig. 5. It can be seen that the

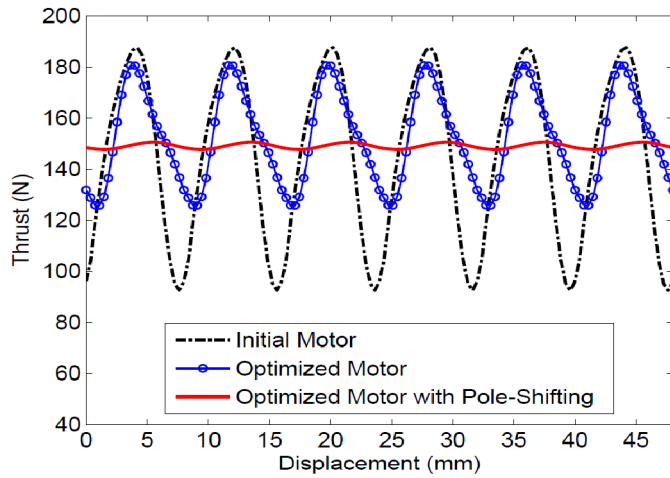


Fig. 4. Thrust force as a function of armature position.

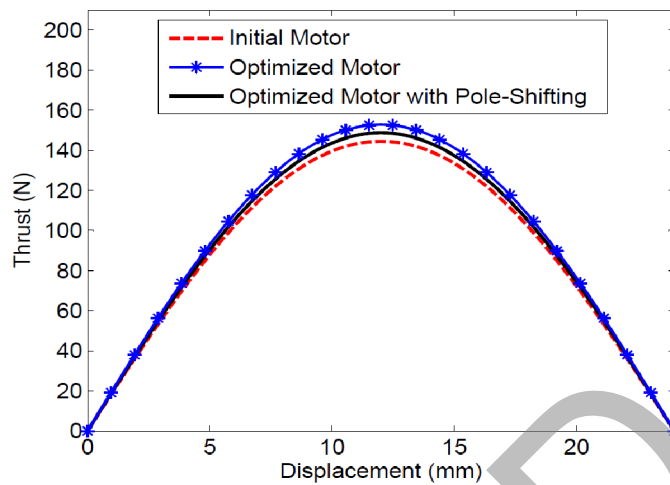


Fig. 5. Thrust characteristic of analyzed motors.

Table V. Design evaluation of analyzed motors.

Parameter (unit)	Original model	Optimized model	Optimized model after pole-shifting
Thrust (N)	144.5	152.8	148.7
Thrust ripple (N) (Peak to peak)	100.2	60.4	4.9
Motor volume (cm^3)	403.98	382.79	382.79
Thrust density (N/cm^3)	0.3577	0.3992	0.3885

average thrust force at full load increases by 8.3N in the optimized configuration with respect to original model while with pole-shifting it increases by 4.2N.

V. CONCLUSION

In this paper, a design optimization method is proposed to achieve higher force density and low thrust ripple in the slotted permanent magnet linear synchronous motor. The results show that an increase of force density by 11.6% and a reduction of thrust ripple by 39.72% in the optimized motor with respect to original one; additionally, after applying pole-shifting to optimal design, force density increased by 8.61% and thrust fluctuation reduced by 95.11% in comparison with initial model. The design method has been verified by time-

stepping transient finite-element method to demonstrate its effectiveness for the improvement of SPMLSM performance in the industrial applications.

REFERENCES

- [1] G. Gieras and Z. J. Piech, *Linear Synchronous Motors*. Boca Raton, FL: CRC, 2000.
- [2] A. Boldea and S. Nasar, *Linear Electromagnetic Devices*. New York: Taylor & Francis, 2001.
- [3] N. R. Tavana, and A. Shoulaie, "Analysis and design of magnetic pole shape in linear permanent-magnet machine," *IEEE Trans. Magn.*, vol.46, no.4, pp.1000-1006, Apr. 2010.
- [4] C. Jiong-jiong, L. Qinfen, H. Xiaoyan, and Y. Yunyue, "Thrust ripple of a permanent magnet LSM with step skewed magnets," *IEEE Trans. Magn.*, vol.48, no.11, pp.4666-4669, Nov. 2012.
- [5] H. Chang-Chou, L. Ping-Lun, and L. Cheng-Tsung, "Optimal design of a permanent magnet linear synchronous motor with low cogging force," *IEEE Trans. Magn.*, vol.48, no.2, pp.1039-1042, Feb. 2012.
- [6] N. R. Tavana, A. Shoulaie, and V. Dinavahi, "Analytical modeling and design optimization of linear synchronous motor With stair-step-shaped magnetic poles for electromagnetic launch applications," *IEEE Trans. Plasma Sci.*, vol.40, no.2, pp.519-527, Feb. 2012.
- [7] J. Wang, G. W. Jewell, and D. Howe, "A general framework for the analysis and design of tubular linear permanent magnet machines," *IEEE Trans. Magn.*, vol. 35, no. 3, pp. 1986-2000, May 1999.
- [8] J. Wang and D. Howe, "Design optimization of radially magnetized, iron-cored, tubular permanent magnet machines and drive systems," *IEEE Trans. Magn.*, vol. 40, no. 5, pp. 3262-3277, Sep. 2004.
- [9] S. Vaez-Zadeh and A. H. Isfahani, "Multiobjective design optimization of air-core linear permanent-magnet synchronous motors for improved thrust and low magnet consumption," *IEEE Trans. Magn.*, vol. 42, no. 3, pp. 446-452, Mar. 2006.
- [10] G. Liuzzi, S. Lucidi, F. Parasiliti, and M. Villani, "Multiobjective optimization techniques for the design of induction motors," *IEEE Trans. on Magn.*, vol.39, no.3, pp. 1261-1264, May. 2003.
- [11] N. Bianchi, S. Bolognani, and A. D. F. Cappello, "Reduction of cogging force in PM linear motors by pole-shifting," *IEE Proc. Electr. Power Appl.*, vol.152, no.3, pp. 703-709, 6 May 2005.